IEEE Access
Multidisciplinary ⋮ Rapid Review ⋮ Open Access Journal

Received May 21, 2020, accepted June 1, 2020, date of publication June 4, 2020, date of current version June 17, 2020.

Digital Object Identifier 10.1109/ACCESS.2020.2999927

Robot Manipulator Calibration Using a Model Based Identification Technique and a Neural Network With the Teaching Learning-Based Optimization

PHU-NGUYEN LE[1] AND HEE-JUN KANG[2]
[1]Graduate School of Electrical Engineering, University of Ulsan, Ulsan 680-749, South Korea
[2]School of Electrical Engineering, University of Ulsan, Ulsan 680-749, South Korea

Corresponding author: Hee-Jun Kang (hjkang@ulsan.ac.kr)

This research was supported by Basic Science Research Program through the National Research Foundation of Korea (NRF) funded by the Ministry of Education (2019R1D1A3A03103528).

ABSTRACT This paper proposes a new calibration method for enhancing robot positional accuracy of the industrial manipulators. By combining the joint deflection model with the conventional kinematic model of a manipulator, the geometric errors and joint deflection errors can be considered together to increase its positional accuracy. Then, a neural network is designed to additionally compensate the unmodeled errors, specially, non-geometric errors. The teaching-learning-based optimization method is employed to optimize weights and bias of the neural network. In order to demonstrate the effectiveness of the proposed method, real experimental studies are carried out on HH 800 manipulator. The enhanced position accuracy of the manipulator after the calibration confirms the feasibility and more positional accuracy over the other calibration methods.

INDEX TERMS Neural network, robot accuracy, robot calibration, teaching-learning-based optimization.

I. INTRODUCTION

Robot manipulators are broadly employed in industry to attain many duties such as welding, painting, pick and place task, etc. The construction of robot manipulators is characterized using their kinematic model parameters. However, in producing and assembly, many errors arise that could not be taken into accounts by the nominal geometric model. For that reason, there is a demand to create model-based robotic calibrations that depend on an error model that symbolizes the connection between the errors of geometric parameters and the arm's tip positioning errors. There are many researchers work on this approach [1], [2]. Numerous studies have been carried out to investigate the suitable geometric model for the robot calibration. Denavit, Hartenberg at el. suggested the DH model that is one of the most fundamental geometric calibration methods. The model has been extensively adopted by researchers [3]–[5]. Gupta proposed another model using the zero-reference position model [6]. This model has been used by some authors [38], [39]. Besides, researchers also proposed many others approaches. Zhuang *et al.* proposed a complete model for completely expressing the geometric and movement of the robotic manipulator of the robot (CPC) by using the singularity-free line representation [7], [8]. Another approach that has been widely examined is the product of exponentials model (POE). The method based on skew theory that allows a global description of robotic motion [9], [10], [11], [40]. There have been some attempts to replace the least square estimation with the Kalman filter, particle filter, etc. [42], [43], [45]–[48] However, the effectiveness of those attempt does not seem to be much. The model-based access has many benefits. It is potential to find out the model parameters precisely in considering that error sources are suitability described by the error model. By using this access, geometric errors can be formed accurately. For instance, the kinematic model and the joint stiffness of the robot are modeled efficiently by many researchers [12], [13], [14]. Geometric error calibration methods have abundant abilities: reducing the calibration time, easy to covert, contributing exactly the information of error's sources. However, they

The associate editor coordinating the review of this manuscript and approving it for publication was Yangmin Li.

also have some drawbacks. Practically, it is difficult to create kinematic identification models that consider all the causes engendering the end effecter error.

The kinematic calibration has been researched for decades and gradually mature. For further accuracy, non-geometric calibration methods have been recently developed, [15]–[25]. Using the non-geometric error approach, some authors employ optimization methods to optimize the robot parameters [15]–[22]. Some studies take the radial basis function [23], [24] or artificial neural network (NN) [25] to generate a connection between the arm's tip position errors and the matching joint angle configurations [25], [27]–[29]. Among them, the back propagation neural network (BPNN) [36] has been widely used due to its capabilities such as learning, adaptation, and approximating any nonlinear function with arbitrary precision [26]. However, the conventional BPNN has a problem in which the performance relies heavily on the input data and hardly finding the overall minima [30]. Numerous methods are suggested to overcome these drawbacks of the BPNN. Heuristic optimization methods are carried on optimizing the structure of the NN. Some of them are particle swam optimization, genetic algorithm, teaching learning optimization, firefly optimization [31]–[34].

In 2011, Rao *et al.* proposed the teaching-learning-based optimization (TLBO) [35]. Overall, the TLBO method replicates the teaching and learning of human. It has two main phases: (1) select the nominate with the best performance to be the teacher of the class to activate the teacher learning step (2). The other nominates are students. They learn from each other and from the teacher. In every interaction, the best solution will become the teacher and the students will change itself base on the teacher and the other students. The TLBO approach is described as a feasible and strong method. It supplies the fast convergence time and easy to get the overall minima.

In this study, the kinematic parameters and joint compliance parameters of the robot are simultaneously identified first by our model-based calibration [12]. However, there are still some unmodeled errors such as friction, thermal variety, gear errors. Then, a proposed neural network with TLBO is applied to compensate the remain errors. For better compensation, the teaching-learning-based-optimization(TLBO) is employed to optimize the weight and bias of the neural network. Finally, the proposed algorithm is implemented for the experimental studies on a HH800 robot. The enhanced position accuracy of the manipulator after the calibration confirms the feasibility and more positional accuracy over the other calibration methods. The proposed method is a combination of model-based and ANN methods which is used the TLBO technique to determine the weight and bias. By using TLBO neural network, the proposed calibration method seems to quite easily reach the global minima. Therefore, the TLBO neural network can be said to have better convergence capability than the traditional backpropagation NN. Furthermore, most of ANN-based technique is applied after the kinematic calibration. Our calibration method simultaneously calibrates both the kinematic errors and joint compliances. The model-based compensation part is the extension to the closed-chain manipulator of our previous work for simple serial robot [12]. After the simultaneous calibration, the TLBO-NN based compensation is accomplished for the un-modelled non-geometric errors. The combination of simultaneous hybrid calibration with a TLBO based neural network is shown to lead to the better capability of reducing the errors of the robot than other calibration methods. Furthermore, the proposed calibration method utilizes the advantages of the TLBO neural network over the conventional back propagation neural network such as better error reducing capability and better global minimum reaching capability.

II. KINEMATIC STRUCTURE OF THE HH800 ROBOT

HH800 is a 6 DOF robot that has a single closed-chain mechanism (2 DOF) [12], [15], [25]. Its sketch and nominal parameters are shown in Fig. 1 and Table 1, respectively.

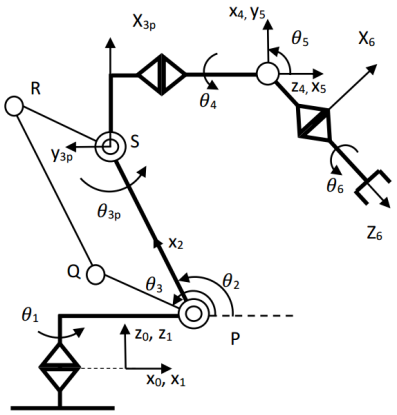

FIGURE 1. Sketch of the HH800 robot.

TABLE 1. Nominal D-H parameters of the Hyundai robot HH800.

D-H parameters of the main open chain						
i	$\alpha_{i-1}(deg)$	$a_{i-1}(m)$	$\beta_{i-1}(deg)$	$b_{i-1}(m)$	$d_i(deg)$	$\theta_i(deg)$
1	0	0	0	0	0	θ_1
2	90	0.515	-	-	0	θ_2
3	0	1.6	0	-	0	θ_3
4	90	0.35	-	-	1.9	θ_4
5	-90	0	-	-	0	θ_5
6	90	0	-	-	0.445	θ_6
T	-	-0.45	-	0.11	0.930	-
Link lengths of the closed loop						
$L_5(m)$		0.8	$L_4(m)$	1.6	$L_3(m)$	0.8

The transformation matrix between the base frame and the tip frame of the robot is expressed:

$$ {}^{0}_{\mathrm{E}}\boldsymbol{T} = {}^{0}_{1}\boldsymbol{T}(\theta_1){}^{1}_{2}\boldsymbol{T}(\theta_2){}^{2}_{3\mathrm{p}}\boldsymbol{T}(\theta_{3p}){}^{3\mathrm{p}}_{4}\boldsymbol{T}(\theta_4){}^{4}_{5}\boldsymbol{T}(\theta_5){}^{5}_{6}\boldsymbol{T}(\theta_6){}^{6}_{\mathrm{E}}\boldsymbol{T} \quad (1) $$

The transformation matrix between the end effector frame and frame 6:

$$ ({}^{6}_{T})\mathbf{T} = \mathbf{T}r_X(a_6)\mathbf{T}r_Y(b_6)\mathbf{T}r_Z(d_7) \quad (2) $$

The closed loop PQRS could be assumed as a parallel planar mechanism. The passive joint position θ_{3p} is calculated as follow [25]:

$$\theta_{3p} = \theta_3 - \theta_2 - 90 \tag{3}$$

III. SIMULTANEOUS IDENTIFICATION JOINT COMPLIANCE AND KINEMATIC PARAMETERS

In a robot static configuration, a robot joint torque causes a twist deformation about a rotation shaft (which represents the entire drive train from the motor to the associated robot link). Therefore, the shaft can be considered as a torsional spring in the compliance modeling. This study investigates characteristics of a torsion spring because they are related to modeling of rotational joint compliance. The characteristics of torsion springs are basically presented by non-linear functions, for example, $T = k_1 * \delta\theta + k2 * (\delta\theta)^3$, where T is the spring torque, ΔP_{extra} is the spring rotational deformation. When the robot joint deformation is small, the linear part becomes dominant. Now, we can assume that the functional relationship between the joint torque and its deformation is linear in this calibration process.

Accepting the manipulator joint can be demonstrated as a linear torsional spring, the joint stiffness value of the i_{th} joint is symbolized by a constant value k_i. Considering the manipulator joint is much bender than the relative link. Hence, the most elastic errors are result of the elasticity of manipulator joints under the effect of the links' weight themselves and external payload. The shifting of the i_{th} joint can be expressed by the effective torques [44]:

$$\Delta\theta_{ci} = \frac{\tau_i}{k_i} = \tau_i c_i \tag{4}$$

The end effector position errors due to the elastic of the joints can be calculated as:

$$\Delta\mathbf{P}_c = \mathbf{J}_\theta \Delta\theta_c = (\mathbf{J}_\theta \tau)\,\mathbf{C} \tag{5}$$

where $\mathbf{C} = [c_1 c_2 \cdots c_n]^T$ is the joint compliance vector, $\Delta\theta_c = [\Delta\theta_{c_1} \Delta\theta_{c_2} \cdots \Delta\theta_{c_n}]^T$ is the joint deflection vector, and $\tau = diag(\tau_1, \tau_2, \cdots, \tau_n)$ is the effective torque in the robot joints at the balance position. J_θ the sub-matrices computed by the method presented in [41]The arm's tip position vector can be formed:

$$\mathbf{P}_{real} = \mathbf{P}_{kin} + \Delta\mathbf{P}_{kin} + \Delta\mathbf{P}_c + \Delta\mathbf{P}_{extra} \tag{6}$$

where $\mathbf{P}_{kin}$ is the result of forward kinematics based on the current kinematic parameters. $\Delta\mathbf{P}_{kin}$, $\Delta\mathbf{P}_c$, $\Delta\mathbf{P}_{extra}$ are the position errors due to the kinematic parameter error, joint elastic, and the residual errors due to the unmodeled sources, respectively. A study that can be utilized for simultaneous recognition joint compliance and kinematic parameters has been proposed by Zhou *et al.* [12]. The combined error model can be showed as:

$$\begin{aligned}\Delta\mathbf{X} &= \Delta\mathbf{P}_{kin} + \Delta\mathbf{P}_c \\ &= \mathbf{J}\Delta\phi + \mathbf{J}_\theta \Delta\theta_c \\ &= \mathbf{J}\Delta\phi + \mathbf{J}_\theta \mathbf{C}\tau \\ &= [\mathbf{J} \quad \mathbf{J}_\theta \tau] \begin{bmatrix} \Delta\phi \\ \mathbf{C} \end{bmatrix} \\ &= \mathbf{J}_\Phi \Delta\Phi \end{aligned} \tag{7}$$

where $\Delta\mathbf{X}$ is a (3×1) vector of three position errors of the robot end-effector. $\mathbf{J}$ is a $(3 \times p)$ matrix that relates the column vectors $\Delta\mathbf{X}$ and $\Delta\mathbf{P}_{kin}$.($p = 27$ is the total number of kinematic parameters). By using the least-square method, the kinematic and joint compliance parameter can be computed at the same time.

IV. ERROR COMPENSATION WITH TLBO BASED NN

The calibration process that is shown in the previous part is effective. However, it does not have any capability to decrease the position errors $\Delta\mathbf{P}_{extra}$ that cannot be negligible. This happens due to unmodeled errors such as friction, thermal variety, gear errors. To lower the residual errors, the additional error compensation technique should be devised such as a neural network, a special function network. In here, a TLBO based neural network is employed to reduce the residual errors. The TLBO algorithm is used to optimize the weight and bias of the neural network and shows the better performance over the conventional back propagation algorithm in this calibration process. The details of this are shown as follows.

First, the robot geometry and joint compliance are simultaneously identified by the Equation 7. By using the least square method, the geometric errors $\Delta\phi$ and the compliance parameters $\mathbf{C}$ are identified. $\Delta\mathbf{P}$ is a (3×1) total position error vector, expressed as:

$$\Delta\mathbf{P} = \Delta\mathbf{P}_{kin} + \Delta\mathbf{P}_c + \Delta\mathbf{P}_{extra} \tag{8}$$

$\Delta\mathbf{P}_{kin}$, $\Delta\mathbf{P}_c$ is calculated by compensation for link geometry and joint compliance errors. The residual position error is $\Delta\mathbf{P}_r$.

$$\Delta\mathbf{P}_r = \mathbf{P}_m - \mathbf{P}_{kin} - \Delta\mathbf{P}_{kin} - \Delta\mathbf{P}_c \tag{9}$$

In this study, the NN optimized by TLBO is used to compensate this residual error. It concludes six inputs representing the joint configurations $\theta_n = [\theta_1, \theta_2, \ldots, \theta_6]$, three outputs representing the residual position errors after the robot geometric and joint angle deflection adjustment. There are 5 nodes in the hidden layer.

When an input pattern p is applied to the NN, the output of each unit j is described by:

$$o_{pj} = \sum_{i=1}^{N} f(w_{ji}x + b_j) \tag{10}$$

where o_{pj} is the output of unit j as a result of the application of input x, w_{ji} is the weight of the node, and b_j is the bias of the unit j. The function f is the activation function, such as a sigmoid, tan-sigmoid, or linear function.

The error in the output layer is given as follows:

$$\mathbf{e} = \Delta\mathbf{P}_r - \mathbf{P}_{nn} \tag{11}$$

where ΔP_r and P_{nn} are the desired and actual output of the neural network. The total mean square error in the output layer is given as follows:

$$\mathbf{E} = \frac{1}{m}\sum_{k=1}^{m}\mathbf{e}_k^2 \tag{12}$$

where m = 3 is the number of nodes in the output layer.

The TLBO is adopted in the error compensation algorithm for the better optimized weights and biases of the neural network. The TLBO method [34], [35], [37] is a recently reported heuristic optimizing method that replicates the teaching and learning of human and is said to be better performance than the conventional back propagation method. The TLBO has two main phases: the teacher phase and the learner phase. In the teacher phase, the candidate with the best performance is selected to be the teacher of the class to activate the teacher learning step. The teacher shares its knowledge to all the learner and increase their performance. In the student phase, the students learn from each other and from the teacher. In every interaction, the best solution will become the teacher and the students will change itself based on the teacher and the other students. The details of this method are fully described by Nayak *et al.* [34]. In this study, the TLBO is applied to optimize the weight and bias of the NN. The process is briefly described as following:

A. TEACHER PHASE

In the teacher phase, the candidate with the best performance is selected to be the teacher applying the mean squared error cost function in Eq. (12). Assume $\mathbf{X}_i = \{x_{i_1}, x_{i_2}, \ldots, x_{i_n}\}$ is the position of the i-th learner that represents the set i of weights and biases of the NN. The mean position of the current class is called $\mathbf{X}_{mean}$ and the best position of the current teacher is noted as $\mathbf{X}_{teacher}$. The teacher phase is expressed as the following equation:

$$\mathbf{X}_{new,i} = \mathbf{X}_{old,i} + rand * (\mathbf{X}_{teacher} - TF * \mathbf{X}_{mean}) \tag{13}$$

where $\mathbf{X}_{new,i}$ and $\mathbf{X}_{old,i}$ are the new and old positions of the ith learner. $\mathbf{X}_{teacher}$ is the position of the current teacher and *rand* is a random number within the range [0, 1]. *TF* is the teaching factor. It is set to 1 or 2 randomly. All the learners should be re-evaluated in this phase. If $\mathbf{X}_{new,i}$ has a higher performance than $\mathbf{X}_{old,i}$ then $\mathbf{X}_{new,i}$ will be chosen and will replace $\mathbf{X}_{old,i}$, otherwise $\mathbf{X}_{old,i}$ is not changed.

B. LEARNER PHASE

For each ith learner in this phase, another learner kth (i $\neq$ k) is randomly selected from the class. The learning process is shown by the following equation:

$$\mathbf{X}_{new,i} = \begin{cases} \mathbf{X}_{old,i} + rand() * (\mathbf{X}_{old,i} - \mathbf{X}_{old,k}) * \\ \mathbf{X}_{old,i} + rand() * (\mathbf{X}_{old,k} - \mathbf{X}_{old,i}) * * \end{cases}$$
$$* : Iff\,(\mathbf{X}_{old,i}) < f(\mathbf{X}_{old,k})$$
$$** : otherwise \tag{14}$$

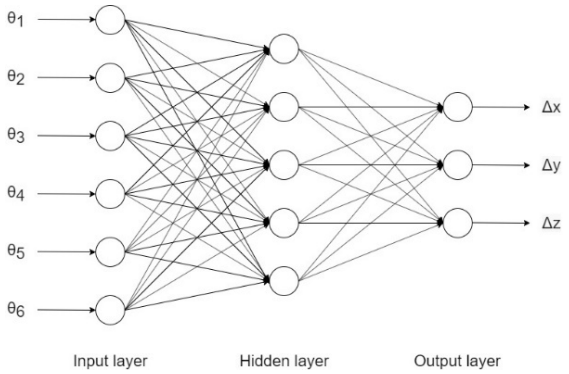

FIGURE 2. Structure of the TLBO-BPNN.

If $\mathbf{X}_{new,i}$ has a higher performance than $\mathbf{X}_{old,i}$ then $\mathbf{X}_{new,i}$ will be selected and $\mathbf{X}_{old,i}$ will be get rid of, otherwise $\mathbf{X}_{old,i}$ is not changed.

In the following step, the stop conditions are checked. If they are satisfied, then the process is stopped. The weights and biases of the NN are set following the $\mathbf{X}_{teacher}$. The process of optimizing the NN using the TLBO is shown in Fig. 3

Overall, the proposed method is shown by the flowchart in the Figure 4:

V. EXPERIMENT AND VALIDATION RESULTS

To clarify the feasibility and efficiency of the proposed method, the proposed calibration method is employed to calibrate a HH800 robot. In addition to verify the effectiveness of the method, results of the calibration process are validated by another set of configurations that is not used for calibration working. Moreover, the proposed technique is compared with other calibration methods to show its capability. The conventional kinematic calibration method (KM), the simultaneous identification of joint compliance and kinematic parameters method (SKCM)[12], and the combination of NN compensator and SKCM method (NN-SKCM) [25] are used to compare with the proposed method (TLBO-NN-SKCM) in both calibration and validation process.

A. EXPERIMENTAL CALIBRATION RESULTS

In the calibration process, the HH800 robot with a heavy load (745 kg), an API laser tracker and an accompanying laser reflector are used to perform the calibration process. The API laser tracker has the accuracy of 0.01 mm/m, repeatability of ±0.006 mm/m. The reflector is fixed at a particular location of the robot end-effector. In order to acquire suitable measurement data for robot parameter identification and weights and bias of the NN determining, the robot moves its end-effector to positions that entirely cover the workspace. The 3D coordinates of the end effector are measured by the Laser Tracker and saved in a computer. At the same time, the associated robot joint readings are also recorded. These measurements will be randomly grouped in three sets. A set of 40 robot configurations (Q1) is used in parameter identification.

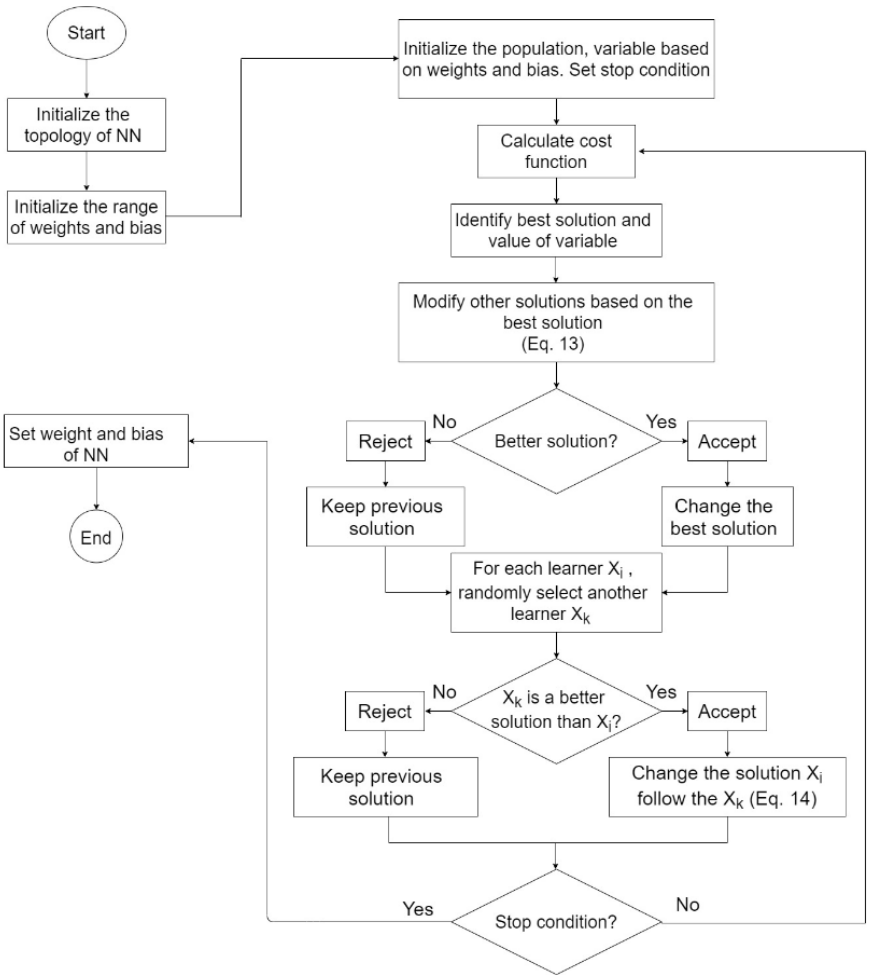

FIGURE 3. Algorithm flow chart of the TLBO to optimize weights and bias of the NN.

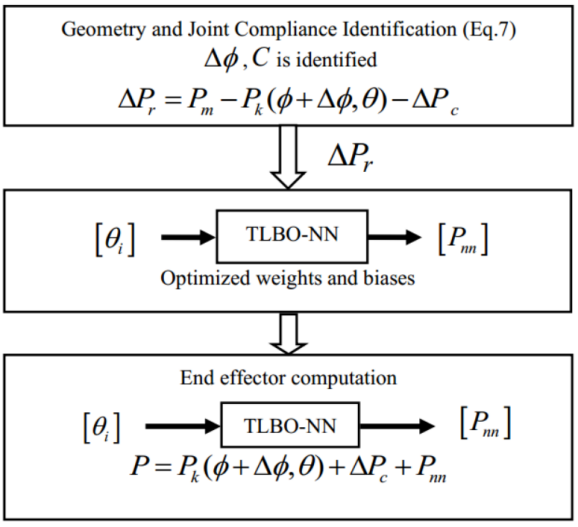

FIGURE 4. Flow chart of the proposed calibration algorithm.

TABLE 2. Stiffness identification (without measurement noise).

	K_2	K_3	K_4	K_5
Stiffness	6.159*10^7	4.388*10^6	3.151*10^6	2.220*10^6

TABLE 3. Nominal D-H parameters of the Hyundai robot HH800.

D-H parameters of the main open chain						
i	$\alpha_{i-1}(deg)$	$a_{i-1}(m)$	$\beta_{i-1}(deg)$	$b_{i-1}(m)$	$d_i(deg)$	$\theta_i(deg)$
1	0.8752	0.0003	0.006	0.0001	0.0976	0.3468
2	89.9412	0.5157	-	-	0(X)	-0.8836
3	0.0133	1.5998	0.001	-	-0.0014	-1.2385
4	90.1172	0.3545	-	-	1.8862	3.3033
5	-90.038	0.0002	-	-	4.087e-05	2.5786
6	90.0371	0.0003	-	-	0.445(X)	0(X)
T	-	-0.4511	-	0.0111	0.9279	-
Link lengths of the closed loop						
$L_5(m)$	0.7996	$L_4(m)$	1.601	$L_3(m)$	0.8(X)	

("-": unavailable, "X": un-identifiable)

By utilizing the SKCM method, the kinematic and joint compliance parameters are identified. These parameters are presented in Table 2 and Table 3 including 4 joint compliance parameters and 29 kinematic parameters. Another set (Q_2) of 50 robot configurations is also randomly selected to determine the weights and biases of the neural network that has

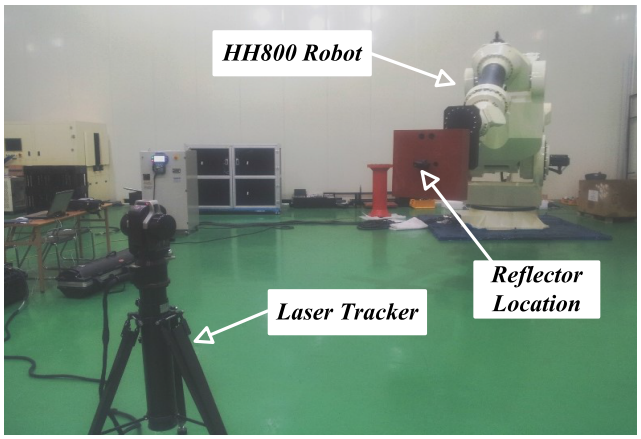

FIGURE 5. Calibration setup of the Hyundai HH800 robot.

5 hidden nodes, 6 inputs and 3 outputs. The reason why we use the different set (Q2) from the set(Q1) is that the neural network compensator has more general error compensation capability over the entire robot workspace. Then, the TLBO is employed to generate the optimized weights and biases of the neural network. The system is arranged as shown in Fig. 5. This offline optimizing process is clearly described in the section IV and also described by the Fig. 3.

The calibration processes of the robot are performed with the 4 different calibration methods such as KM [3]–[5], SKCM [12], and NN-SKCM [25] and the proposed TLBO-NN-SKCM. Their results are shown in the Table 4.

TABLE 4. Absolute position accuracy of the HH800 robot (calibration).

	Mean (mm)	Maximum (mm)	Std. (mm)
Nominal robot model	4.0654	6.3291	0.8803
KM	0.9076	3.7486	0.7671
SKCM	0.8370	2.7578	0.5461
NN- SKCM	0.4650	1.0123	0.1967
After proposed technique	0.3945	0.6544	0.1717

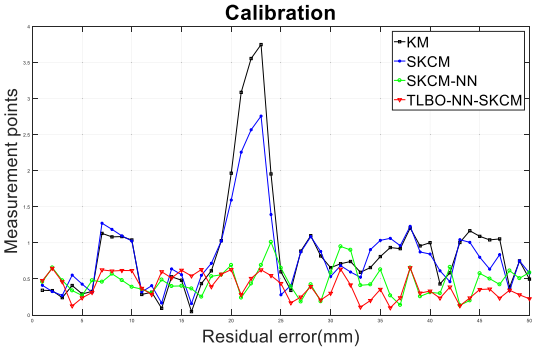

FIGURE 6. Absolute position error of the HH800 robot after calibration.

The results in Table 4 and Fig. 6 show that the proposed method achieve the best performance over other methods. The Figure 6 provides a visual result of the absolute position errors of each calibration pose using 4 calibration methods. It shows that the position errors generated by the proposed method is the lowest and better converging in compare with the other methods. The mean of position errors generated by the proposed method is more precise by 56.53% than the errors by KM method (from 0.9076 mm to 0.3945 mm), by 52.87% than the errors by SKCM method(from 0.8370 mm to 0.3945 mm), and by 15.16% than the errors by NN-SKCM method (from 0.4650 mm to 0.3945 mm). The proposed technique also has the lowest maximum position error as well as the best standard deviation.

B. EXPERIMENTAL VALIDATION RESULTS

From Table 4 and Fig. 6, the proposed method shows its error compensation capability with the positions used in this calibration process. In order to show the general capability over the entire robot workspace, it should be validated with the other data set. The other set of 50 robot configurations (Q3) is randomly selected and the calibration processes are carried out for 4 different methods.

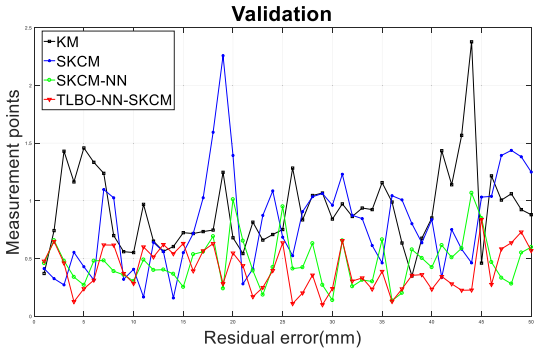

FIGURE 7. Absolute position error of the HH800 robot after validation.

The calibration results with Q3 data set are shown in Table 5 and Fig. 7. The Figure 7 shows the residual error of each poses using 4 methods in the validation process. It is clearly to see from the figure that the proposed method is the best over both the positions used in the calibration process and the general position in overall workspace.

The mean of position errors generated by the proposed method is more precise by 56.03% than the errors by KM method (from 0.9227 mm to 0.4057 mm), by 49.85% than the errors by SKCM method (from 0.8009 mm to 0.4057 mm), and by 13.90% than the errors by NN-SKCM method (from 0.4712 mm to 0.4057 mm). The proposed technique also has the lowest maximum position error as well as the best standard deviation.

C. BETTER CONVERGENCE OF TLBO NEURAL NETWORK

In this calibration process, several data sets of robot configurations are applied to the back propagation neural network and the TLBO neural network. From this implementation experience, while the back propagation neural network seems

TABLE 5. Absolute position accuracy of the HH800 robot (Validation).

	Mean (mm)	Maximum (mm)	Std. (mm)
Nominal robot model	4.0629	6.1681	0.8451
KM	0.9227	2.3769	0.3597
SKCM	0.8009	2.2571	0.4227
NN-SKCM	0.4712	1.0678	0.2087
After proposed technique	0.4057	0.8378	0.1864

TABLE 6. List of notations used in the paper.

Sym.	Meaning
${}^{A}_{B}\boldsymbol{T}$	Transformation matrix between the frame A and frame B
θ_x	Position of joint x
k_i	Joint stiffness value of the i_{th} joint
$\Delta\theta_c$	Joint deflection vector
τ	Effective torque in the robot joints at the balance position
C	Joint compliance vector
$\mathbf{P}_{real}$	End effector position vector
$\mathbf{P}_{kin}$	Result of forward kinematics
$\Delta\mathbf{P}_{kin}$	Position errors due to the kinematic parameter error
$\Delta\mathbf{P}_{c}$	Position errors due to the joint elastic
$\Delta\mathbf{P}_{extra}$	Residual position errors due to the unmodeled sources
$\Delta\mathbf{X}$	Vector of three position errors of the robot end-effector
$\mathbf{J}$	Matrix that relates the ΔP_{kin} and $\Delta\mathbf{X}$
$\mathbf{J}_\theta$	Sub-matrices that relates the τ and $\Delta\theta_c$
$\Delta\phi$	Vector of kinematic errors
$\Delta\mathbf{P}$	Total position error vector
$\mathbf{P}_m$	Position of the end effector by measuring
$\Delta\mathbf{P}_r$	Residual position errors
o_{pj}	Output of unit j as a result of the application of input x
w_{ji}	Weight of the node
b_j	Bias of the unit j
f	Activation function
$\mathbf{P}_{nn}$	Output of the neural network
$\mathbf{E}$	Total mean square error
$\mathbf{X}_i$	Position of the i-th learner
$\mathbf{X}_{mean}$	Mean position of the current class
$\mathbf{X}_{teacher}$	Position of the current teacher
$\mathbf{X}_{old,i}$	Old positions of the i*th* learner
$\mathbf{X}_{new,i}$	New positions of the *ith* learner

to be easily got into the local minima and to need reiteration by randomly resetting the weights and biases to reach the global minima, the TLBO neural network seems to quite easily reach the global minima. Therefore, the TLBO neural network can be said to have better convergence capability.

VI. CONCLUSIONS

In this study, a new calibration method with an error compensating TLBO neural network is proposed for enhancing robot positional accuracy of the industrial manipulators. By combining the joint deflection model with the conventional kinematic model of a manipulator, the geometric errors and joint deflection errors can be simultaneously considered to increase its positional accuracy. Then, a neural network is designed to additionally compensate the unmodeled errors, specially, non-geometric errors. The teaching-learning-based optimization(TLBO) method is employed to optimize weights and biases of the neural network. In order to demonstrate the effectiveness of the proposed method, real experimental studies are carried out on the HH 800 manipulator. The enhanced position accuracy of the manipulator after the calibration confirms the feasibility and more positional accuracy over the other calibration methods. Additionally, the adopted TLBO neural network can be said to have better convergence capability than the back propagation neural network in this calibration process. This advantage allows that the proposed method is more feasible in real offline programming environment.

REFERENCES

[1] C. Brisan and M. Hiller, "Aspects of calibration and control of PARTNER robots," in *Proc. IEEE Int. Conf. Autom., Qual. Test., Robot.*, Cluj-Napoca, Romania, May 2006, pp. 272–277.

[2] R. Manne, "Analysis of two PLS algorithms for multivariate calibration," *Chemo. Intell. Lab. Syst.*, vol. 2, pp. 187–197, Aug. 1987.

[3] J. J. Craig, *Introduction to Robotics: Mechanics and Control*, 2nd ed., Reading, MA, USA: Addison-Wesley, 1989, pp. 68–77.

[4] S. Hayati and M. Mirmirani, "Improving the absolute positioning accuracy of robot manipulators," *J. Robotic Syst.*, vol. 2, no. 4, pp. 397–413, 1985.

[5] S. Hayati, K. Tso, and G. Roston, "Robot geometry calibration," in *Proc. IEEE Int. Conf. Robot. Autom.*, Philadelphia, PA, USA, vol. 1, Apr. 1988, pp. 947–951.

[6] K. C. Gupta, "Kinematic analysis of manipulators using the zero reference position description," *Int. J. Robot. Res.*, vol. 5, no. 2, pp. 5–13, Jun. 1986.

[7] H. Zhuang, Z. S. Roth, and F. Hamano, "A complete and parametrically continuous kinematic model for robot manipulators," in *Proc. IEEE Int. Conf. Robot. Autom.*, Cincinnati, OH, USA, vol. 1, May 1990, pp. 92–97.

[8] H. Zhuang, L. K. Wang, and Z. S. Roth, "Error-model-based robot calibration using the modified CPC model," *Int. J. Robot. Comp. Integr. Manufact.*, vol. 10, no. 4, pp. 287–299, Aug. 1993.

[9] K. Okamura and F. C. Park, "Kinematic calibration using the product of exponentials formula," *Robotica*, vol. 14, no. 4, pp. 415–421, Jul. 1996.

[10] G. Chen, L. Kong, Q. Li, H. Wang, and Z. Lin, "Complete, minimal and continuous error models for the kinematic calibration of parallel manipulators based on POE formula," *Mechanism Mach. Theory*, vol. 121, pp. 844–856, Mar. 2018.

[11] G. Chen, H. Wang, and Z. Lin, "Determination of the identifiable parameters in robot calibration based on the POE formula," *IEEE Trans. Robot.*, vol. 30, no. 5, pp. 1066–1077, Oct. 2014.

[12] J. Zhou, H.-N. Nguyen, and H.-J. Kang, "Simultaneous identification of joint compliance and kinematic parameters of industrial robots," *Int. J. Precis. Eng. Manuf.*, vol. 15, no. 11, pp. 2257–2264, Nov. 2014.

[13] C. Dumas, S. Caro, S. Garnier, and B. Furet, "Joint stiffness identification of six-revolute industrial serial robots," *Robot. Comput.-Integr. Manuf.*, vol. 27, no. 4, pp. 881–888, Aug. 2011.

[14] C. Lightcap, S. Hamner, T. Schmitz, and S. Banks, "Improved positioning accuracy of the PA10-6CE robot with geometric and flexibility calibration," *IEEE Trans. Robot.*, vol. 24, no. 2, pp. 452–456, Apr. 2008.

[15] A. Martinelli, N. Tomatis, A. Tapus, and R. Siegwart, "Simultaneous localization and odometry calibration for mobile robot," in *Proc. IEEE/RSJ Int. Conf. Intell. Robots Syst. (IROS)*, Las Vegas, NV, USA, vol. 2, Oct. 2003, pp. 1499–1504.

[16] Y. Song, J. Zhang, B. Lian, and T. Sun, "Kinematic calibration of a 5-DoF parallel kinematic machine," *Precis. Eng.*, vol. 45, pp. 242–261, Jul. 2016.
[17] J.-M. Renders, E. Rossignol, M. Becquet, and R. Hanus, "Kinematic calibration and geometrical parameter identification for robots," *IEEE Trans. Robot. Autom.*, vol. 7, no. 6, pp. 721–732, Dec. 1991.
[18] J. Swevers, C. Ganseman, D. B. Tukel, J. de Schutter, and H. Van Brussel, "Optimal robot excitation and identification," *IEEE Trans. Robot. Autom.*, vol. 13, no. 5, pp. 730–740, Oct. 1997.
[19] Z. Jiang, W. Zhou, H. Li, Y. Mo, W. Ni, and Q. Huang, "A new kind of accurate calibration method for robotic kinematic parameters based on the extended Kalman and particle filter algorithm," *IEEE Trans. Ind. Electron.*, vol. 65, no. 4, pp. 3337–3345, Apr. 2018.
[20] J. Zhou and H. J. Kang, "A hybrid least-squares genetic algorithm–based algorithm for simultaneous identification of geometric and compliance errors in industrial robots," *Adv. Mech. Eng.*, vol. 7, no. 6, pp. 1–12, Jun. 2015.
[21] A. Li, D. Wu, and Z. Ma, "Robot calibration based on multi-thread particle swarm optimization," in *Proc. 6th IEEE Int. Conf. Ind. Informat.*, Daejeon, South Korea, Jul. 2008, pp. 454–457.
[22] X. Xie, Z. Li, and G. Wang, "Manipulator calibration based on PSO-RBF neural network error model," in *Proc. AIP Conf.*, Malang City, Indonesia, 2018, pp. 020–026.
[23] J. H. Jang, S. H. Kim, and Y. K. Kwak, "Calibration of geometric and non-geometric errors of an industrial robot," *Robotica*, vol. 19, no. 3, pp. 311–321, May 2001.
[24] P. Y. Tao and G. Yang, "Calibration of industrial robots with product-of-exponential (POE) model and adaptive neural networks," in *Proc. IEEE Int. Conf. Robot. Autom. (ICRA)*, Seattle, WA, USA, May 2015, pp. 1448–1454.
[25] H.-N. Nguyen, P.-N. Le, and H.-J. Kang, "A new calibration method for enhancing robot position accuracy by combining a robot model–based identification approach and an artificial neural network–based error compensation technique," *Adv. Mech. Eng.*, vol. 11, no. 1, Jan. 2019, Art. no. 168781401882293, doi: 10.1177/1687814018822935.
[26] M. R. Baker and R. B. Patil, "Universal approximation theorem for interval neural networks," *Rel. Comp.*, vol. 4, no. 3, pp. 235–239, Aug. 1998.
[27] G. Gao, F. Liu, H. San, X. Wu, and W. Wang, "Hybrid optimal kinematic parameter identification for an industrial robot based on BPNN-PSO," *Complexity*, vol. 2018, pp. 1–11, Jul. 2018, doi: 10.1155/2018/4258676.
[28] Z. Wang, Z. Chen, Y. Wang, C. Mao, and Q. Hang, "A robot calibration method based on joint angle division and an artificial neural network," *Math. Problems Eng.*, vol. 2019, pp. 1–12, Mar. 2019, doi: 10.1155/2019/9293484.
[29] N. Takanashi, "6 DOF manipulators absolute positioning accuracy improvement using a neural-network," in *Proc. IEEE Int. Workshop Intell. Robots Syst., Towards New Frontier Appl.*, Ibaraki, Japan, Jul. 1990, pp. 635–640.
[30] X. G. Wang, Z. Tang, H. Tamura, M. Ishii, and W. D. Sun, "An improved backpropagation algorithm to avoid the local minima problem," *Neurocomputing*, vol. 56, pp. 455–460, Jan. 2004.
[31] D.-S. Wang and X.-H. Xu, "Genetic neural network and application in welding robot error compensation," in *Proc. Int. Conf. Mach. Learn. Cybern.*, vol. 7, Guangzhou, China, Aug. 2005, pp. 4070–4075.
[32] G. Jiang, M. Luo, K. Bai, and S. Chen, "A precise positioning method for a puncture robot based on a PSO-optimized BP neural network algorithm," *Appl. Sci.*, vol. 7, no. 10, p. 969, Sep. 2017, doi: 10.3390/app7100969.
[33] Y. Zhang, Z. Jin, and Y. Chen, "Hybrid teaching–learning-based optimization and neural network algorithm for engineering design optimization problems," *Knowl.-Based Syst.*, vol. 187, Jan. 2020, Art. no. 104836, doi: 10.1016/j.knosys.2019.07.007.
[34] J. Nayak, B. Naik, D. Pelusi, and A. V. Krishna, "A comprehensive review and performance analysis of firefly algorithm for artificial neural networks," in *Nature-Inspired Computation in Data Mining and Machine Learning*. Cham, Switzerland: Springer, 2020, pp. 137–159.
[35] R. V. Rao, V. J. Savsani, and D. P. Vakharia, "Teaching–learning-based optimization: A novel method for constrained mechanical design optimization problems," *Comput.-Aided Des.*, vol. 43, no. 3, pp. 303–315, Mar. 2011.
[36] D. E. Rumelhart, G. E. Hinton, and R. J. Williams, "Learning internal representations by error propagation," in *Parallel Distributed Processing—Explorations in the Microstructure of Cognition*. vol. 1. Cambridge, MA, USA: MIT Press, 1986.
[37] F. Zou, L. Wang, X. Hei, and D. Chen, "Teaching–learning-based optimization with learning experience of other learners and its application," *Appl. Soft Comput.*, vol. 37, pp. 725–736, Dec. 2015.
[38] L.-P. Cheng and K. Kazerounian, "Study and enumeration of singular configurations for the kinematic model of human arm," in *Proc. IEEE 26th Annu. Northeast Bioeng. Conf.*, Storrs, CT, USA, Apr. 2000, pp. 3–4.
[39] B. W. Mooring, "An improved method for identifying the kinematic parameters in a six-axis robot," in *Proc. Comput. Eng. Conf. Exhib.*, Las Vegas, NV, USA, 1984, pp. 79–84.
[40] H. Wang, X. Lu, W. Cui, Z. Zhang, Y. Li, and C. Sheng, "General inverse solution of six-degrees-of-freedom serial robots based on the product of exponentials model," *Assem. Autom.*, vol. 38, no. 3, pp. 361–367, Aug. 2018.
[41] Y. Nakamura and M. Ghodoussi, "Dynamics computation of closed-link robot mechanisms with nonredundant and redundant actuators," *IEEE Trans. Robot. Autom.*, vol. 5, no. 3, pp. 294–302, Jun. 1989.
[42] G. Du, P. Zhang, and X. Liu, "Markerless human–manipulator interface using leap motion with interval Kalman filter and improved particle filter," *IEEE Trans. Ind. Informat.*, vol. 12, no. 2, pp. 694–704, Apr. 2016.
[43] G. Du and P. Zhang, "A markerless human–robot interface using particle filter and Kalman filter for dual robots," *IEEE Trans. Ind. Electron.*, vol. 62, no. 4, pp. 2257–2264, Apr. 2015.
[44] J. Craig, *Introduction to Robotics: Mechanics and Control*, 2nd ed. Boston, MA, USA: Addison-Wesley, 1989.
[45] H.-N. Nguyen, J. Zhou, and H.-J. Kang, "A calibration method for enhancing robot accuracy through integration of an extended Kalman filter algorithm and an artificial neural network," *Neurocomputing*, vol. 151, pp. 996–1005, Mar. 2015.
[46] Z. Jiang, W. Zhou, H. Li, Y. Mo, W. Ni, and Q. Huang, "A new kind of accurate calibration method for robotic kinematic parameters based on the extended Kalman and particle filter algorithm," *IEEE Trans. Ind. Electron.*, vol. 65, no. 4, pp. 3337–3345, Apr. 2018, doi: 10.1109/TIE.2017.2748058.
[47] W. He, C. Xue, X. Yu, Z. Li, and C. Yang, "Admittance-based controller design for physical human-robot interaction in the constrained task space," *IEEE Trans. Autom. Sci. Eng.*, early access, Apr. 21, 2020, doi: 10.1109/TASE.2020.2983225.
[48] X. Yu, W. He, H. Li, and J. Sun, "Adaptive fuzzy full-state and output-feedback control for uncertain robots with output constraint," *IEEE Trans. Syst., Man, Cybern. Syst.*, early access, Feb. 3, 2020, doi: 10.1109/TSMC.2019.2963072.

PHU-NGUYEN LE received the B.S. degree in electrical engineering from the Da Nang University of Technology, Da Nang, Vietnam, in 2012. He is currently pursuing the Ph.D. degree with the School of Electrical Engineering, University of Ulsan, Ulsan, South Korea. His research interests include sensor-based robotic applications, robot calibration, and artificial intelligent-based robotic calibration.

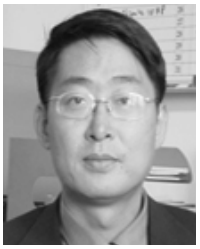

HEE-JUN KANG received the B.S. degree in mechanical engineering from Seoul National University, South Korea, in 1985, and the M.S. and Ph.D. degrees in mechanical engineering from The University of Texas at Austin, Austin, TX, USA, in 1988 and 1991, respectively. Since March 1992, he has been a Professor of electrical engineering with the University of Ulsan. His current research interests are sensor-based robotic application, robot calibration, haptics, robot fault diagnosis, and mechanism analysis.